The Complex Double Gaussian Distribution

Nicholas O'Donoughue, *Student Member, IEEE,* and José M.F. Moura, *Fellow, IEEE,*

Abstract—We present the *complex Double Gaussian* distribution that describes the product of two independent, non-zero mean, complex Gaussian random variables, a doubly-infinite summation of terms. This distribution is useful in a wide array of problems. We discuss its application to blind TR detection systems by deriving the Neyman-Pearson optimal detector when the channel is modeled as the product of two independent complex Gaussian random variables, such as in a Time Reversal scenario. We show that near-optimal detection performance can be achieved with as few as 25 summation terms. Theoretical analysis and Monte Carlo simulations illustrate our results.

Index Terms—Complex Gaussian, Complex Double Gaussian, Detection, Time Reversal, Probability Distribution of Product of Gaussian Variables

I. INTRODUCTION

In [1], we presented the probability distribution function (PDF) for the product of two non-zero mean complex Gaussian random variables. We refer to it as the *complex Double Gaussian* PDF. This PDF is useful in many practical applications. The *keyhole* or *pinhole* channel model proposed in [2] describes a system where both the transmitter and the receiver are surrounded by multipath scattering and all communication between them passes through a single waveguide, such as the corner of a building. In this scenario, the channel is the product of two complex Gaussian random variables. In time reversal [3], a source first probes the channel, which is collected, time reversed (or phase conjugated), and retransmitted back to the original source. If this channel experiences Rayleigh fading, then the aggregate channel response is the product of two complex Gaussians. Finally, in many communication systems the received signal is sent through a linear combiner consisting built from a channel estimate generated from pilot symbols. Under Rayleigh fading, the output of this combiner is the product of complex Gaussian random variables. In all three of these scenarios, and many others, the *complex Double Gaussian* distribution can be a useful tool for design and analysis.

In this paper, we present the *complex Double Gaussian* PDF, which is computed via a doubly-infinite summation, whose terms include modified Bessel functions of the first and second kind. We also apply it to blind TR, see [4]. We use the *complex Double Gaussian* distribution to design the binary hypothesis test deriving the Neyman-Pearson optimal detector. We verify theoretically the performance of our detector using Monte Carlo simulations and compare its performance to an Energy Detector.

N. O'Donoughue and J.M.F. Moura are with the Department of Electrical and Computer Engineering, Carnegie Mellon University, 5000 Forbes Ave, Pittsburgh, PA 15217. {nodonoug,moura}@ece.cmu.edu

We present the PDF for the *complex Double Gaussian* distribution in Section II. The Blind TR Detection System is described in Section III, where we also derive the optimal detector. Simulation results are presented in Section IV, followed by our conclusion in Section V.

II. DOUBLE GAUSSIAN PDF

If $X \sim \mathcal{CN}\left(\nu_x e^{j\phi_x}, \sigma_x^2\right)$ (meaning that X is a Complex Gaussian random variable with mean $\nu_x e^{j\phi_x}$ and variance σ_x^2) and $Y \sim \mathcal{CN}\left(\nu_y e^{j\phi_y}, \sigma_y^2\right)$ are independent random variables, then the product $Z = XY$ is characterized by the polar distribution:

$$f_{\Theta_z, R_z}(\theta_z, r_z) = \frac{2r_z}{\pi \sigma_x^2 \sigma_y^2} e^{-\left(k_x^2 + k_y^2\right)} \tag{1}$$

$$\sum_{n,p=0}^{\infty} \frac{1}{n!p!} \left(\frac{\alpha}{2\cos\left(\theta_z - \phi_x - \phi_y\right)}\right)^{n+p}$$

$$\left(\frac{k_x}{k_y}\right)^{n-p} K_{n-p}\left(\frac{2r_z}{\sigma_x \sigma_y}\right) I_{n+p}(2\alpha),$$

where:

$$\alpha = \sqrt{2r_z k_x k_y \cos\left(\theta_z - \phi_x - \phi_y\right)/\sigma_x \sigma_y} \tag{2}$$

$$k_x = \frac{\nu_x}{\sigma_x} \tag{3}$$

$$k_y = \frac{\nu_y}{\sigma_y}. \tag{4}$$

The detailed proof of (1) is exceedingly tedious. An abridged version of the proof is presented in [1], Appendix A. The proof begins by computing the joint distribution of the output phase Θ_z and input amplitudes R_x and R_y. Then, a transformation of variables from R_x and R_y to R_z and a dummy variable T is conducted. Finally, the variable T is integrated out. This integration process is extremely involved and requires the use of several Bessel Function identities and expansions found in [5], as well as several complicated integrations obtained using results in [6]. If the two inputs are both zero-mean ($\nu_x = \nu_y = 0$), then (1) reduces to [1]:

$$f_{R_z, \Theta_z}(r_z, \theta_z) = \frac{2r_z}{\pi \sigma_x^2 \sigma_y^2} K_0\left(\frac{2r_z}{\sigma_x \sigma_y}\right). \tag{5}$$

Comments regarding (1): We call this result the *complex Double Gaussian* distribution and use the shorthand $\mathcal{CNN}$ to refer to it:

$$Z \sim \mathcal{CNN}\left(\nu_x e^{j\phi_x}, \sigma_x^2; \nu_y e^{j\phi_y}, \sigma_y^2\right). \tag{6}$$

The first two moments of (1) are given by:

$$E[Z] = E[X]E[Y] = \nu_x \nu_y e^{j(\phi_x + \phi_y)} \tag{7}$$

$$\text{Var}[Z] = \text{Var}[X]\text{Var}[Y] = \sigma_x^2 \sigma_y^2. \tag{8}$$

Complex Double Gaussian PDF
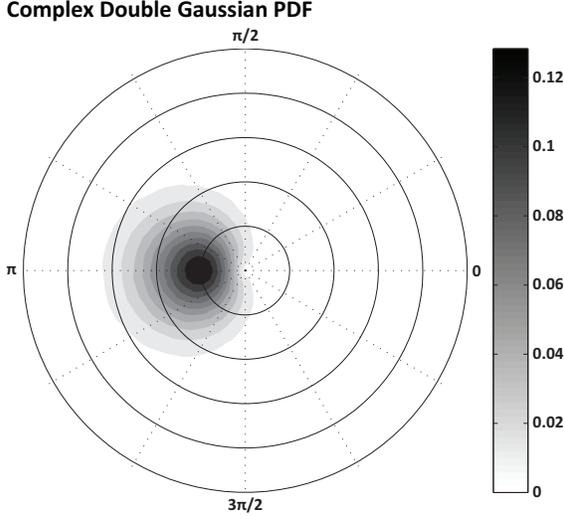

Fig. 1. Plot of the two-dimensional PDF $f_{R_z,\Theta_z}(r_z,\theta_z)$, described in (1), for $k_x = 1, k_y = 1/\sqrt{2}$ and $\phi_x = \phi_y = \pi/2$.

Likewise, higher order moments of Z are obtained from the first two moments of X and Y.

The infinite summations over n and p arise from the Rician k-factors k_x and k_y, respectively. These terms express the relative strength of the deterministic components of X and Y. If one of k_x or k_y is zero, the corresponding sum across n or p, respectively, becomes superfluous and the PDF reduces to a single summation. If both are zero, then the summation in (1) reduces to a single term.

We plot an example of (1) in Figure 1 for the case where $k_x = 1$, $k_y = 1/\sqrt{2}$, $\sigma_x^2 = 1$ $\sigma_y^2 = 1/2$, and $\phi_x = \phi_y = \frac{\pi}{2}$. This plot was generated using 100 summation terms ($n = 0, \ldots, 9$, $p = 0, \ldots, 9$). The plot exhibits a cardioid shape, this is because we are plotting the polar form of the two-dimensional PDF $f_{R_z,\Theta_z}(r_z,\theta_z)$. A simple conversion to Cartesian coordinates would remove the hole that appears at the origin.

III. BLIND TIME REVERSAL DETECTION

We consider the detection of a target in the presence of stationary random multipath scattering, this application is briefly discussed in the recently submitted manuscript [1], but we present here a more in-depth analysis. We will utilize a Time Reversal detection strategy similar to the one outlined in [3], [4] with one notable difference. In the detection system we consider here, the Time Reversal mirror will not communicate with the detector. Thus, the detection system must operate without knowledge of the result of the forward transmission. The meaning of this statement will be clarified below.

We define the frequency samples ω_q, $q = [0, Q-1]$. We model the target as a point target with a deterministic response T. For the clutter, we utilize the Wise-Sense Stationary Uncorrelated Scattering (WSSUS) model for multipath propagation [7]. WSSUS assumes that the multipath response comes from a linear superposition of uncorrelated echoes, and that each echo is characterized by a WSS impulse response.

From this, is follows that the clutter is drawn from a zero-mean complex Gaussian distribution with power spectral density (PSD) $P_c(\omega_q)$. This channel model is discussed in detail in [8] and was used in [4]. We transmit the probing signal $S(\omega_q)$ and write the response:

$$Y(\omega_q) = [T + C(\omega_q)] S(\omega_q) + V(\omega_q), \qquad (9)$$

where $C(\omega_q) \sim \mathcal{CN}(0, P_c(\omega_q))$ is the clutter response, and $V(\omega_q) \sim \mathcal{CN}(0, \sigma_v^2)$ represents additive noise. For simplicity, we use a white probing signal:

$$S(\omega_q) = \sqrt{E_s/Q}, \qquad (10)$$

for some transmit power E_s. The Time Reversal probing signal is generated using a scaled, phase-conjugated version of the received signal $Y(\omega_q)$:

$$S_{TR}(\omega_q) = kY^*(\omega_q), \qquad (11)$$

where k is the energy normalization factor defined by:

$$k = \sqrt{\frac{E_s}{\sum_{q=0}^{Q-1} |Y(\omega_q)|^2}}. \qquad (12)$$

We assume that k is approximately deterministic, as was argued in [9]. The Time Reversal probing signal $S_{TR}(\omega_q)$ is distributed as a complex Gaussian:

$$S_{TR}(\omega_q) \sim \mathcal{CN}\left(kT^*, k^2\left(P_c(\omega_q)\frac{E_s}{Q} + \sigma_v^2\right)\right). \qquad (13)$$

The signal $S_{TR}(\omega_q)$ is then transmitted from the receiver back to the source, where the received signal is:

$$Y_{TR}(\omega_q) = \left(T + \overline{C}(\omega_q)\right) S_{TR}(\omega_q) + \overline{V}(\omega_q), \qquad (14)$$

where $\overline{C}(\omega_q)$ is the clutter channel for the second transmission, and $\overline{V}(\omega_q)$ is the noise signal for the second transmission. We assume that the clutter and noise signals are independent of each other and independent from one transmission to the next. This assumption will be valid if there is sufficient time delay between the forward and TR transmission stages, relative to the coherence time of the clutter channel. If we ignore the noise term, then (14) is distributed according to the product of independent Complex Gaussians:

$$Y_{TR}(\omega_q) \sim \mathcal{CNN}\left(\mu_{x,q}, \sigma_{x,q}^2; \mu_{y,q}, \sigma_{y,q}^2\right), \qquad (15)$$
$$\mu_{x,q} = T,$$
$$\mu_{y,q} = kT^*,$$
$$\sigma_{x,q}^2 = P_c(\omega_q),$$
$$\sigma_{y,q}^2 = k^2\left(P_c(\omega_q)\frac{E_s}{Q} + \sigma_v^2\right).$$

At this stage, we set up the binary hypothesis test. The detectors in [3] were designed to use both $Y(\omega_q)$ and $Y_{TR}(\omega_q)$. In this application, however, we consider the case where $Y(\omega_q)$ is not available to the detector. In the null hypothesis, the case where no target is present, $T = 0$, and $Y_{TR}(\omega_q)$ is distributed according to (5). In the alternative hypothesis, $T > 0$, and $Y_{TR}(\omega_q)$ is distributed according to (1). Thus:

$$\begin{aligned} \mathbb{H}_0 &: \ \mu_{x,q} = 0, \ \mu_{y,q} = 0 \\ \mathbb{H}_1 &: \ \mu_{x,q} = T, \ \mu_{y,q} = kT^* \end{aligned} \qquad (16)$$

A. Likelihood Ratio Test

To compute the likelihood ratio test statistic, we utilize the mean and variance parameters given in (15). We divide the distribution under $\mathbb{H}_1$, given by (1), by the distribution under $\mathbb{H}_0$, given by (5). The result is given:

$$\ell_q = \prod_{q=0}^{Q-1} e^{-\left(k_{x,q}^2 + k_{y,q}^2\right)} \sum_{n,p=0}^{N-1} \frac{1}{n!p!} \left(\frac{\alpha}{2\cos(\theta_q)}\right)^{n+p}$$

$$\left(\frac{k_{x,q}}{k_{y,q}}\right)^{n-p} \frac{K_{n-p}\left(\frac{2r_q}{\sigma_{x,q}\sigma_{y,q}}\right)}{K_0\left(\frac{2r_q}{\sigma_{x,q}\sigma_{y,q}}\right)} I_{n+p}(2\alpha), \qquad (17)$$

where $\theta_q = \angle Y_{TR}(\omega_q)$, $r_q = |Y_{TR}(\omega_q)|$, and $\alpha_q = \sqrt{2r_q k_{x,q} k_{y,q} \cos(\theta_q)}/\sigma_{x,q}\sigma_{y,q}$. The summations over n and p are both carried out for the first N terms, instead of to ∞, resulting in a total of N^2 summation terms. Unless otherwise specified, we will utilize $N = 15$ in our simulations. It would be possible to construct the likelihood ratio ℓ numerically, through a Monte Carlo simulation, but that approach would be much more computationally complex, and would not yield the analytical representation in (17). From the likelihood ratio ℓ, we can construct the test [10]:

$$\phi = \begin{cases} 1 & \ell \geq \ell_0 \\ 0 & \ell < \ell_0 \end{cases}, \qquad (18)$$

for some threshold ℓ_0. Ideally, we would use the distribution of the test statistic ℓ to determine the appropriate threshold ℓ_0 for some desired false alarm rate. However, its distribution is unknown, so we must rely on Monte Carlo simulations to determine the appropriate threshold.

IV. Monte Carlo Simulations

To test the detector derived in Section III, we construct a simulation scenario wherein the clutter channel follows a Gaussian power spectral density in the band 2-4GHz, and the target (a point target) has a constant value $T = e^{j\pi/2}$. We confine our transmit power to the $E_s = 1$, and vary the total clutter power $E_c = \sum_{q=0}^{Q-1} P_c(\omega_q)$. We vary the number of frequency samples Q and conduct $MC = 10^6$ Monte Carlo trials for each scenario.

Using these Monte Carlo trials, we set the probability of false alarm to $(P_{FA}) = 0.01$, determine the appropriate threshold from a noise-only simulation, and then use that threshold to compute the probability of detection (P_D) for the likelihood ratio test given in (18) as we vary the number of frequencies Q and the signal-to-noise ratio SNR. The signal-to-noise ratio is defined:

$$\text{SNR}_{\text{dB}} = 10 \log_{10}\left(\frac{E_s |T|^2}{Q\sigma_v^2}\right). \qquad (19)$$

We also define the signal-to-clutter ratio SCR_{dB}:

$$\text{SCR}_{\text{dB}} = 10 \log_{10}\left(\frac{Q|T|^2}{\sum_{q=0}^{Q-1} P_c(\omega_q)}\right). \qquad (20)$$
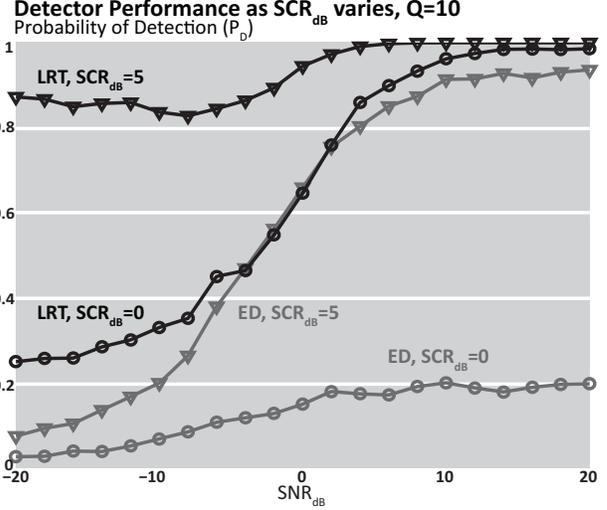

Fig. 2. Plot of the detector performance for the Likelihood Ratio Test (LRT) detailed in (17) and the Energy Detector (ED) in (21) when the false alarm rate is fixed at $P_{FA} = 0.01$ and $Q = 10$ frequency samples.
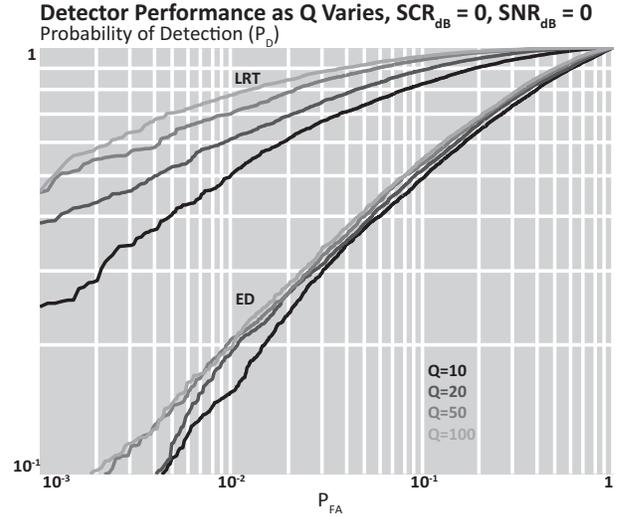

Fig. 3. Plot of the detector performance for the Likelihood Ratio Test (LRT) detailed in (17) and the Energy Detector (ED) in (21) for various values of Q when $\text{SCR}_{\text{dB}} = 0$ and $\text{SNR}_{\text{dB}} = 0$.

For comparison, we also computed the receiver operating characteristics of an energy detector:

$$\ell_{ED} = \sum_{q=0}^{Q-1} |Y_{TR}(\omega_q)|^2. \qquad (21)$$

For the first test, we compare the likelihood ratio test (LRT) that we derived in (17) to the Energy Detector in (21) with varying SCR. We plot the results in Figure 2, which depicts Probability of Detection for each scenario against SNR_{dB}. We consider two scenarios: strong clutter ($\text{SCR}_{\text{dB}} = 0$) and weak clutter ($\text{SCR}_{\text{dB}} = 5$). In the strong clutter case, the ED fails to distinguish the target, while the LRT achieves $P_D > .9$ at high SNR. In the weak clutter case, the ED improves and

Detector Performance as N Varies, SCR$_{dB}$=0, Q=10
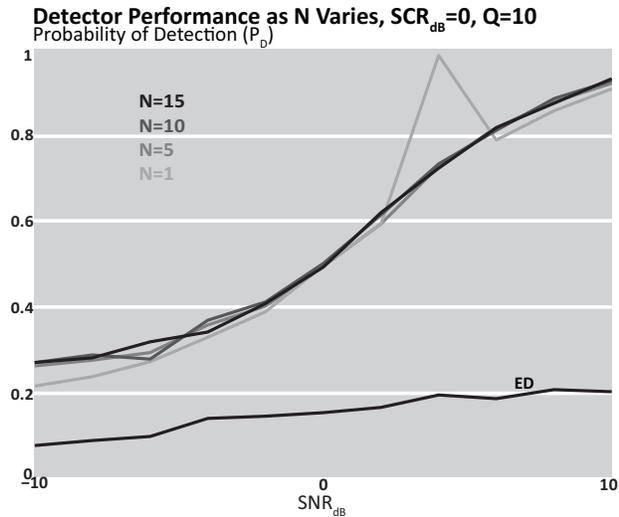Probability of Detection (P$_D$)

Fig. 4. Plot of the detector performance for the Likelihood Ratio Test (LRT) detailed in (17) and the Energy Detector (ED) in (21) for various summation lengths (N) when the false alarm rate is fixed at $P_{FA} = 0.01$, $Q = 10$ frequency samples, and $\text{SCR}_{dB} = 0$.

performs similarly to the LRT detector in strong clutter. The LRT improves as well, outpacing the ED. From this test, we can see that the LRT has a distinct SCR advantage over the ED, since it utilizes the distribution of $Y_{TR}(\omega_q)$.

For the second test, we set the signal-to-clutter ratio to a fixed value of $\text{SCR}_{dB} = 0$ and the signal-to-noise ratio to a fixed value of $\text{SNR}_{dB} = 0$. We allow the number of frequencies Q to take on the values $Q = 10$, 20, 50, and 100. The results are plotted in Figure 3, on a log-log scale with probability of detection (P_D) ranging from 0.1 to 1 and probability of false alarm (P_{FA}) ranging from 10^{-3} to 1. From this plot, we can see that the LRT performance increases notably with increasing Q, while the ED improves marginally by comparison. For example, if we set the false alarm rate to $P_{FA} = 10^{-2}$, the ED will achieve $\approx 15\%$ detection with $Q = 10$ and 20% detection with $Q = 100$, a 33% increase. The LRT, however, achieves $\approx 50\%$ detection with $Q = 10$ and almost 80% with $Q = 100$, a 60% increase. Since the LRT is leveraging more information about the channel and target, it stands to benefit more from a larger sampling space.

A. Effect of Summation Length

The PDF for the *complex Double Gaussian* distribution is a doubly-infinite summation. As a result, the likelihood ratio test statistic presented in (17) also contains a doubly-infinite summation. In order to compute the PDF, this summation must be truncated at some point N. In this test, we look at how the choice of N affects detector performance. In Figure 4, we show the detector performance (P_D vs. SNR_{dB}) for various summation lengths N, when $\text{SCR}_{dB} = 0$ and $Q = 10$. We also plot the performance curve for the ED in this scenario, as a benchmark. We can see from the results that the detector does well with just a single term, except for a spurious result at $\text{SNR}_{dB} = 4$, which can be attributed to numerical

instability of the algorithm when only one term is used. A modest increase to $N = 5$ (25 summation terms) removes the numerical instability but performs only slightly better, and moving to $N = 10$ (100 summation terms) or $N = 15$ (225 summation terms) yields almost no improvement. Thus, for this test scenario, only 25 summation terms are necessary for near-optimal performance.

V. DISCUSSION AND CONCLUSION

We present the *complex Double Gaussian* distribution, a recently derived result. In this paper, we show the usefulness of this distribution by applying it to the problem of a Blind TR Detection scheme. We use this distribution to characterize the aggregate channel response and derive the optimal detector in a Neyman-Pearson sense. We verify our results with Monte Carlo simulations and compare them to an energy detector. We also show that near-optimal detection performance can be achieved with as few as 25 terms from the doubly infinite summation that makes up the likelihood ratio test statistic. In addition to the application that we present here, an important problem that can benefit from the *complex Double Gaussian* distribution is error analysis in communication systems that rely on a linear combiner, such as M-ary Phase Shift Keying (M-PSK) systems [11]. The output of the linear combiner can be characterized as the product of two complex Gaussian random variables. This allows the *complex Double Gaussian* distribution to be used for analysis, such as computing the Symbol Error Probability (SEP). This problem was considered in detail in [1].

REFERENCES

[1] N. O'Donoughue and J. M. F. Moura, "On the product of independent complex Gaussians," *submitted to Signal Processing, IEEE Transactions on*, 2011.

[2] D. Gesbert, H. Bolcskei, D. Gore, and A. Paulraj, "Outdoor MIMO wireless channels: models and performance prediction," *Communications, IEEE Transactions on*, vol. 50, no. 12, pp. 1926 – 1934, Dec 2002.

[3] Y. Jin and J. M. F. Moura, "Time-reversal detection using antenna arrays," *Signal Processing, IEEE Transactions on*, vol. 57, no. 4, pp. 1396 –1414, april 2009.

[4] N. O'Donoughue, J. Harley, and J. M. F. Moura, "Detection of targets embedded in multipath clutter with time reversal," in *Acoustics, Speech and Signal Processing (ICASSP), 2011 IEEE International Conference on*, may 2011, pp. 3868 –3871.

[5] F. W. Oliver, D. W. Lozier, R. F. Boisvert, and C. W. Clark, Eds., *NIST Handbook of Mathematical Functions*. Cambridge University Press, 2010.

[6] I. Gradshteyn and I. Ryzhik, *Tables of Integrals, Series, and Products*. Academic Press, 1980.

[7] J. G. Proakis, *Digital Communications*, 3rd ed. McGraw-Hill, 1995.

[8] S. Kay, "Optimal signal design for detection of Gaussian point targets in stationary Gaussian clutter/reverberation," *Selected Topics in Signal Processing, IEEE Journal of*, vol. 1, no. 1, pp. 31 –41, june 2007.

[9] Y. Jin, J. M. F. Moura, and N. O'Donoughue, "Time reversal in multiple-input multiple-output radar," *Selected Topics in Signal Processing, IEEE Journal of*, vol. 4, no. 1, pp. 210 –225, feb. 2010.

[10] L. L. Scharf, *Statistical Signal Processing*. Addison-Wesley, 1991.

[11] R. Mallik, "Distribution of inner product of two complex Gaussian vectors and its application to MPSK performance," in *Communications, 2008. ICC '08. IEEE International Conference on*, may 2008, pp. 4616 –4620.